Estimating the role of climate internal variability and source of uncertainties in hydrological climate-impact projections

Wenjun Cai
Taiyuan University of Technology
Jia Liu (liujiaiwhr@163.com)
China Institute of Water Resources and Hydropower Research
Xueping Zhu
Taiyuan University of Technology
Xuehua Zhao
Taiyuan University of Technology

Research Article

Keywords: Climate change, GCMs, hydrological climate-impact projections, uncertainties quantified, CIV, ANOVA

Posted Date: December 29th, 2021

DOI: https://doi.org/10.21203/rs.3.rs-1198481/v1

Estimating the role of climate internal variability and source of uncertainties in hydrological climate-impact projections

Wenjun Cai[1] Jia Liu[2,*] Xueping Zhu[1,*] Xuehua Zhao[1]

1 College of Water Resource and Engineering, Taiyuan University of Technology, Taiyuan 030024, China;

2 State Key Laboratory of Simulation and Regulation of Water Cycle in River Basin, China Institute of Water Resources and Hydropower Research

Abstract: Hydrological climate-impact projections in future are limited by large uncertainties from various sources. Therefore, this study aimed to explore and estimate the sources of uncertainties involved in climate changing impacted assessment in a representative watershed of Northeastern China. Moreover, recent researches indicated that the climate internal variability (CIV) plays an important role in various of hydrological climate-impact projections. Six downscaled Global climate models (GCMs) under two emission scenarios and a calibrate Soil and Water Assessment Tool (SWAT) model were used to obtain hydrological projections in future periods. The CIV and signal-to-noise ratio (SNR) are investigated to analyze the the role of internal variability in hydrological projections. The results shows that the internal variability shows a considerable influence on hydrological projections, which need be partitioned and quantified particularly. Moreover, it worth noting the CIV can propagate from precipitation and ET to runoff projections through the hydrological simulation process. In order to partition the CIV and sources of uncertainties, the uncertainty decomposed frameworks based on analysis of variance (ANOVA) are established. The results demonstrate that the CIV and GCMs are the dominate contributors of runoff in rainy season. In contrast, the CIV and SWAT model parameter sets provided obvious uncertainty to runoff in January to May and October to December. The findings of this study advised that the uncertainty is complex in hydrological simulation process hence, it is meaning and necessary to estimate the uncertainty in climate simulation process, the uncertainty analysis results can provide effectively efforts to reduce uncertainty and then give some positive suggestions to stakeholders for adaption countermeasure under climate change.

Key words: Climate change; GCMs; hydrological climate-impact projections; uncertainties quantified; CIV; ANOVA

1. Introduction

Climate change is expected to impact the precipitation and temperature by the end of the 21st century, the changes in precipitation and temperature may substantially effect the regional and global hydrological cycle, quantifying the response of runoff of climate change is directly associated with water resources management.(Zhang et al. 2016; Wang et al. 2018;Vaghef et al. 2019; Anjum et al. 2019; Yuan et al. 2020). Global climate models (GCMs) are primary tools for providing the future climate variables in changing environment, which can be used to simulated the general circulation of the earth's atmosphere, which can provide the credible information from past to future meteorological data (Zhang et al. 2016). Multi-model ensembles consisting of GCMs were used to drive the hydrological models (HMs) to obtain sreamflow and the other hydrological projections. It is become an useful method to estimate the hydrological process response to climate change in various regions of the world (Champagne et al. 2020). However, lots of uncertainties exist in the simulate process of future hydrological climate-impact projections. The different aspects of uncertainty in the model chain can be categorized as: (I) the internal variability of hydrological climate-impact projections simulation; (II) scenarios uncertainty; (III) model uncertainty (Byun et al. 2019; Li et al. 2015; Chen et al. 2016; Ficklin et al. 2016; Zhang et al. 2013; Lee et al. 2016; Nóbrega et al. 2011; Shen et al. 2018).

Scenarios uncertainty is caused by the highly uncertainty trajectory of future socioeconomic development of human societies and the lack of knowledge of future anthropogentic emission of greenhouse gases (GHG) (Lafaysse et al. 2014). The scenarios uncertainty always shows like the different representative concentration pathway (RCP) emission scenarios for future periods.

Model uncertainty is due to the lack of ability to describe the real geophysical process, and embodied in GCM and HM uncertainties. The GCMs uncertainty mainly comes from the the choice of GCMs. Different GCMs always simulated different climate projections under the same emission scenarios. HMs uncertainty due to the model structure and model parameters.The mathematical formulas of hydrological model can portray the rainfall and runoff physical process of basin, because of the lack of ability to describe the real world process, hydrological model are established by incomplete representations of reality (Gupta A and Govindaraju R S 2019), since, it may result in model structure uncertainty. The contribution of parameters uncertainties is significant impacts in the model output, the different parameters may due to the runoff changing in

62 opposite directions (Zhang et al. 2019). In addition, parameter uncertainty is relatively to control
63 by some conceptual or empirical parameters and an appropriate calibration method (Wu and Chen
64 2015). The inappropriate estimation of main parameters may result in non-negligible uncertainty,
65 for this reason, parameters uncertainty has received most attention of previous studies (Nerantzaki
66 et al. 2019).

67 The climate internal variability (CIV) is the natural variability of the climate system and
68 includes processes intrinstic to the atmosphere, the ocean, the couple ocean-atmosphere system,
69 which is expected to present the natural viability of the regional climate at decadal multi-decadal
70 time scale in the simulation chains (Deser et al. 2012; Lafaysse et al. 2014; Pesce et al. 2019). Due
71 to the chaotic variability of the climate system, the precipitation and temperature simulated by
72 GCMs are influenced by the CIV (Deser et al. 2014). The precipitation and temperature are the
73 important input of hydrological simulation process, hence, the CIV in the climate system are
74 cascading to the hydrological processes (Lafaysse et al. 2014). The uncertainties due to the CIV is
75 the important uncertainty sources in hydrological projections (Hawkins and Sutton 2009).
76 Partitioning and quantifying CIV in a multireplicate multimodel ensemble of
77 hydro-meteorological projections and estimating CIV under different emission scenarios are
78 necessary for provide reliable forecasts and useful decision-making (Lafaysse et al. 2014; Doi and
79 Kim 2020). The internal variability of climate projections has been analyzed by many studies to
80 estimate the uncertainty range of a chosen forced response and obtain a robust detection of climate
81 change effects (Steinschneider et al. 2015; Schindler et al. 2015; Nerantzaki et al. 2020).

82 Generally, the attribute the hydrological climate-impact projections to CIV is a comparative
83 concept of climate external variability affect by anthropogentic or nature change in external
84 forcing (Doi and Kim 2020; Deser et al. 2012; Thompson et al. 2015). Clearly partitioning CIV
85 and external forcing is necessary for hydrological climate-impact projections uncertainties.
86 Although the some source of uncertainties of hydrological climate-impact projections have been
87 estimated in numerous of researches, the CIV, scenarios, model uncertainties need be equally
88 investigate in future literature. The role of the CIV in hydrological climate-impact projections is
89 also rarely investigate.

90 To segregate the sources of uncertainties in hydrological climate-impact projections, Bosshard
91 et al. (2013) quantified the uncertainties contributions of an ensemble of hydrological climate

92 impact projections by using the analysis of variance (ANOVA) method. The ANOVA technique
93 has fewer assumptions as compared to other uncertainty analysis methods, such as Bayesian
94 methods and Generalized Likelihood Uncertainty Estimation (GULE) (Vaghef et al. 2019). In
95 recently hydrological application, the assessment framework based on ANOVA has been used to
96 investigated the individual and interaction uncertainty from different sources (Chawla et al. 2018;
97 Qi et al. 2016; Kujawa et al. 2020; Keller et al. 2019; Wang et al. 2020). However, the different
98 kinds of uncertainty sources have not been estimated equally in previous researches. They mainly
99 aim on decomposition the GCMs, emission scenarios, downscaling method, hydrological model
100 structure and parameter for simulation process (Kujawa et al. 2020; Shi et al. 2020; Keller et al.
101 2019). Moreover, to investigate the role of the internal variability in the overall climate change
102 uncertainty can provide more useful information to uncertainty estimating of simulation process
103 and establish more comprehensive framework of uncertainty analysis (Liu et al. 2012; Xue et al.
104 2014; Yen et al. 2014; Schindler et al. 2015; Steinschneider et al. 2015; Nerantzaki et al. 2020).
105 Therefore, comprehensive and systematical investigating the hydrological climate change impact
106 and estimating different sources of uncertainty is worth and necessary.
107 The purpose of this manuscript is to estimate the contribution of sources of uncertainty and
108 investigate the role of internal variability in hydrological climate-impact projections in a
109 representative watershed of Northeastern China. In order to obtain a robust detection of climate
110 change effects and give some useful suggestions to practical decision making, the hydrological
111 climate-impact projections in this manuscript contained precipitation, temperature, ET and runoff
112 projections under climate change.
113 The mainly aim of this study is: (1) to analyze the seasonal changing of precipitation,
114 temperature, ET and runoff projections under climate change; (2) to partition and quantify the
115 source of uncertainty in hydrological climate-impact projections; (3) to investigate the role of
116 internal variability in the hydrological climate-impact projections; (4) to confirm mainly impact
117 source of uncertainty in hydrological simulation process.The uncertainty decomposition
118 framework of this study shows in Fig.1.。

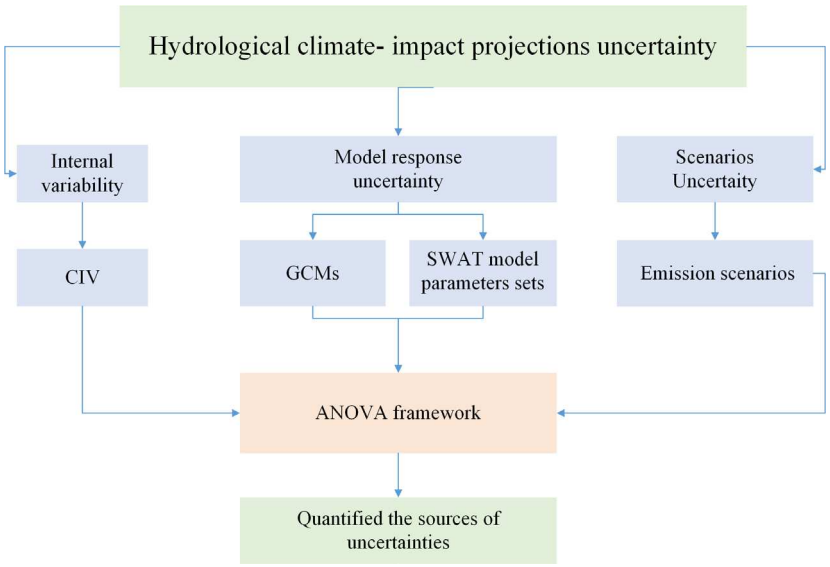

Fig.1. Flowchart of the uncertainty decomposition framework of this study

For this purpose, this manuscript combined six GCMs models under two Representative Concentration Pathways (RCPs), which have been based on the fifth phase of the Coupled Model Intercomparison Project (CMIP5). These climate change scenarios were downscaled by the Morphing method, which use an operation of shift or stretch to downscale the hydrological variability (Belcher et al. 2005). A widely used hydrological model SWAT was used to runoff simulation, the SUFI-2 (Abbaspour et al. 2004, 2007) uncertainty approach for capturing the relatively uncertainty of SWAT model parameters. The findings of this research may provide some meaningful suggestions on hydrological climate change impacts and presents a methodology for partitioning uncertainty sources of runoff projections in a representative watershed in Northeastern of China.

2. Study area and data

2.1. Study area

The Biliu River basin is located in the Northeastern of China spans 39.54° to 40.35° N in latitude and 122.29° to 122.93° E in longitude with an approximate area of 2085km^2 (Fig.2). The Biliu River Reservoir was built in 1975 and the storage of it is 9.34×10^8 m^3. The mainly utility of this reservoir is water supply for nearby big cities and cropland irrigation. Another reservoir, called Yushi Reservoir, which was built in 2001 and located in the upstream of Biliu River, with a storage capacity of 0.89×10^8 m^3 and a drainage area of 313km^2. Because of the reservoir supplies water to the outside of the basin, thus, the impact of Yushi Reservoir should be considered in the

hydrological model. This study area has the characterized of temperate, monsoon marine climate, and with the rainy season from June to September. The mean annual precipitation is 746mm, the average annual temperature is 8.40℃ to 10.3℃, and the maximum and minimum temperatures are 35.8℃and -23.5℃, respectively.

2.2. Data and climate change scenarios

The historical observed daily precipitation and daily runoff data were available form1978-2004, the monthly precipitation and runoff data were form 1958-2011, which were obtain from the Biliu River Reservoir administration and Hydrology Bureau of Liaoning Province. The DEM, land-use map, and soil type map are obtained from the Data Center for Resources and Environmental Science, Chinese Academy of Sciences.

The climate data were used output from six GCMs in CMIP5 under RCP4.5 and RCP8.5 emission scenarios: ACCESS1-0, BCC-CSM1.1(m), CESM1-BGC, CESM1-CAM5, CMCC-CM, MPI-ESM-MR (Table1). The climate data were extracted for 1980-2004 period, 2041-2065 period and 2066-2090 period, which defined as reference period, 2050s and 2080s two future period.

Table 1 Description of CMIP5 climate models and scenarios

Climate Models	Country	Resolution	Scenarios
ACCESS1.0	Australia	$1.88^{\circ} \times 2.48^{\circ}$	RCP4.5, RCP8.5
BCC-CSM1.1(m)	China	$1.13^{\circ} \times 1.13^{\circ}$	RCP4.5, RCP8.5
CESM1(BGC)	USA	$1.3^{\circ} \times 0.9^{\circ}$	RCP4.5, RCP8.5
CESM1(CAM5)	USA	$1.3^{\circ} \times 0.9^{\circ}$	RCP4.5, RCP8.5
CMCC-CM	Italy	$0.75^{\circ} \times 0.75^{\circ}$	RCP4.5, RCP8.5
MPI-ESM-MR	Germany	$1.88^{\circ} \times 1.88^{\circ}$	RCP4.5, RCP8.5

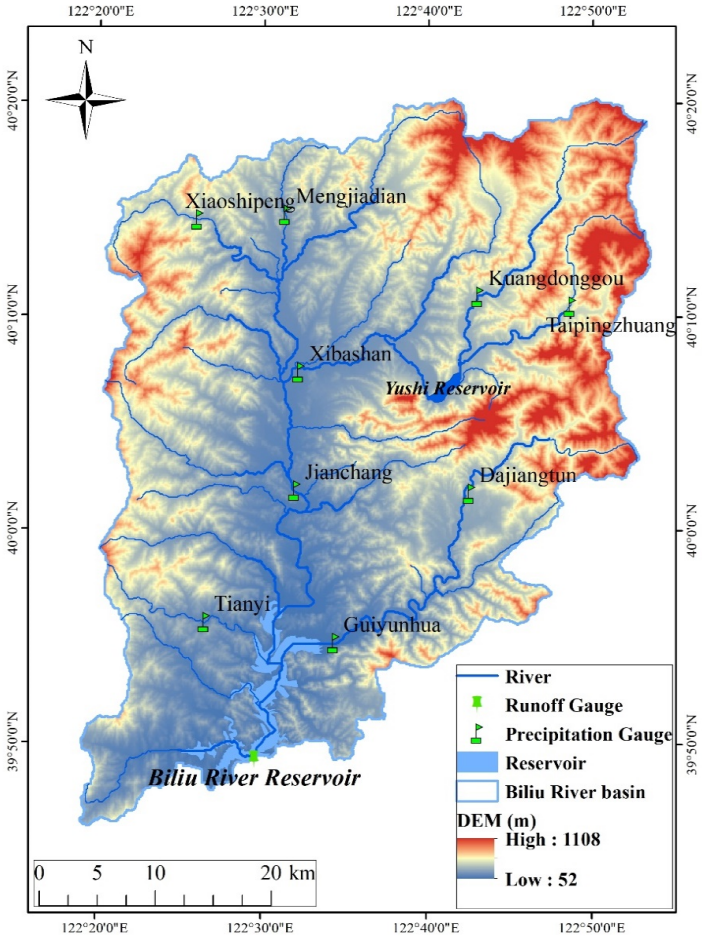

157

158 Fig.2. The location of precipitation gauge, runoff gauge, river, boundaries in Biliu River basin.

159

160 ## 3. Methodology

161 ### 3.1 Hydrological modeling and parameter uncertainty assessment

162 The SWAT 2012 is used to simulate runoff in this study. SWAT is a physically based water-scale

163 model which is widely used in investigating hydrological processes around the world (Wang et al.

164 2020). The model divided the watershed into hydrologic response units (HRUs), each of these

165 HRUs based on a unique combination of soil, land use and slope characteristics (Nie et al. 2011).

166 Recently, the model has been developed to estimate the climate change impact on hydrological

167 regimes in the predict conditions over long periods of future. The SWAT-CUP software was

168 utilized for calibration and uncertainty assessment of parameters (Abbaspour et al. 2007). SUFI2

169 algorithm was chosen to calibrate and validate the parameters in the SWAT-CUP (Abbaspour et al.

170 2004). In order to account for the parameter uncertainty of the model, this manuscript used Latin

171 hypercube sampling (LHS) to generated hydrological model parameter sets. The Nash-Sutcliffe

177 $|Re|$ below 10.

178 3.2 Climate change scenario and downscaling method

179 The CMIP5 have provide future climate database and widely around the world (Kujawa et al.
180 2020; Zhu et al. 2018; Shi et al. 2020). Six GCMs from CMIP5 were selected to represent the
181 future climate scenarios under RCP4.5 and RCP8.5 emission scenarios. SWAT model was driven
182 by six GCMs and two emission scenarios, for a total of 12 ensemble scenario members under
183 2050s and 2080s.

184 Because of the simper and easily using merits (Abbaspour et al. 2004; Zhu et al. 2018; Chen et
185 al. 2010), this manuscript adopts Morphing approach to remove biased from the original GCMs
186 climate projections, this method involves a shift, a linear stretch (scaling factor), and a
187 combination of shift and a stretch (Belcher et al. 2005). The downscaled precipitation and
188 temperature are calculated by Morphing and shows acceptable performance in the study
189 watersheds more details of the downscaling process were shown in Zhu et al. (2018).

190 3.3 Method of the CIV estimation

191 In order to investigate the role of the CIV in hydrological climate-impact projections, the
192 externally forced and internal variability need be partitioned and quantified particularly. Generally,
193 the internal variability is quantified by the “detrend” and “differenced” method, the external
194 forcing is subtracted from the hydrological variable series, and then the fluctuations of the
195 variables are regarded as internal variability (Kim et al. 2018). The average of a large number
196 ensemble members can average out the internal variability, and then the signal remaining is the
197 response of external forcing (Frankcombe et al. 2015). Hence, the internal variability can be
198 obtained by subtracting the model-mean from each ensemble member (Frankcombe et al. 2015).
199 The standard deviation of the ensemble variable or the residual to quantify the internal variability
200 is the robust method has been applied in many previous publications (Yu et al. 2020; Maher et al.

201 2020; Evin et al. 2019; Hingray et al. 2020; Thompson et al. 2015; Lafaysse et al. 2014).

202 $$CIV = \frac{1}{N}\sum_{i=1}^{N}\left(\sqrt{\frac{1}{T-1}\sum_{j=1}^{T}\left(Hc_{i,j} - \overline{Hc_{i,j}}\right)^2}\right) \quad (1)$$

203 Where *i* and *j* is the ensemble number and the individual year; N and T are the total number of
204 ensemble numbers and years, respectively; HC is the month time series of hydrological
205 climate-impact variables.

206 The key of estimating CIV is partitioning the external forcing from the hydrological series, and
207 the standard deviation of the given hydrological climate-impact projections is calculated as
208 internal variability (Evin et al. 2019). The signal-to-noise ratio (SNR) always be used to quantify
209 the relative contributions of internal variability and external forcing (Deser et al. 2014). The SNR
210 can provide useful information to investigate the magnitude of external forcing and internal
211 variability of hydrological climate-impact projections under future climate change. The
212 model-mean of each ensemble is used as signal, and the ensemble average of sum of the squared
213 difference between each member and ensemble mean is defined as noise (Evin et al. 2019). The
214 SNR is defined signal divided by noise.

215 $$nosie = \sqrt{\frac{1}{T(N-1)}\sum_{j=1}^{T}\sum_{i=1}^{N}\left(Hc_{ij} - \overline{Hc_j}\right)^2} \quad (2)$$

216 $$\overline{Hc_j} = \frac{1}{N}\sum_{i=1}^{N} Hc_{ij} \quad (3)$$

217 ### 3.4 Source of uncertainties decomposition

218 (1) The hydrological response to climate change

219 For any hydrological projections obtained from hydrological simulation process for the i^{th}
220 member of and time j^{th}, the raw hydrological projections can be decomposed by hydrological
221 response to climate change and internal vairability (Evin et al. 2019; Hingray et al. 2019). The raw
222 hydrological projections $Y_{i,j}$ under climate change can be express as Eq. (4).

223 $$Y_{i,j} = \varphi_{i,j} + \eta_{i,j} \quad (4)$$

224 Where $\varphi_{i,j}$ is the hydrological response to climate change; $\eta_{i,j}$ is the deviation from the hydrological response
225 obtained with i^{th} member of and time $j^{th.}$ which can also be express as internal variability.

226 (2) Decomposition of the hydrological response to climate change

227 The hydrological response to climate change $\varphi_{i,j}$ of any GCM/emission scenarios can be defined
228 as Eq. (5):

229 $$\varphi_{i,j} = \mu + \alpha_h + \beta_k + \gamma_l + \xi_{h,k,l} \quad (5)$$

230 Where μ is the overall mean of hydrological response to climate change; α_h is the effect contributed by
231 hydrological model parameters; β_k is the effect contribute by GCMs; γ_l is the effect contribute emission scenarios;
232 $\xi_{h,k,l}$ is the interaction terms of the model.

233 (3) The different components of the total uncertainty

234 On the base of the above expression of the raw hydrological response from GCM/emission
235 scenarios, the overall variance of the hydrological projections $Var[Y_{h,k,l}]$ as flowing:

236 $$Var[Y_{h,k,l}] = Var[\varphi_{h,k,l}] + Var[\eta_{h,j,k}] \quad (6)$$

237 Where $Var[\varphi_{h,k,l}]$ is the total uncertainty in hydrological response, $Var[\eta_{h,j,k}]$ is the uncertainty of internal
238 variability of hydrological projections.

239 $$Var[\varphi_{h,j,k}] = Var[\alpha_h] + Var[\beta_j] + Var[\gamma_k] + Var[\xi_{h,j,k}] \quad (7)$$

240 Where $Var[\alpha_h]$ is the variance of SWAT model parameters effects; $Var[\beta_j]$ is the variance of GCMs model
241 effect; $Var[\gamma_k]$ is the variance of the emission scenarios； $Var[\xi_{h,j,k}]$ is the variance of the interaction effects.

242 (4) Source of uncertainties quantifying

243 This manuscript constructs a three-way ANOVA framework to decomposition the different
244 uncertainties contribution, this technology has ability to partition the total observed variance into
245 different sources, and then quantify the contribution of different sources to total variance (Wang et
246 al. 2018; Aryal et al. 2017).

247 It based on a biased variance estimator that underestimates the variance when the sample size is
248 small. In order to diminish the bias effects caused by the different number of levels of the
249 uncertainty factors, Bosshard et al. (2013) proposed a subsampling method was applied in this
250 manuscript. This subsampling technology selected two samples from the large sample sets, and
251 then a new sample can be generated for ANOVA. This manuscript selects two SWAT parameters
252 sets out of the 100 sets, the superscript j was replaced by g(h, i), which is 2×4950 matrix as
253 following:

$$g = \begin{pmatrix} 1 & 1 & \cdots & 1 & 2 & 2 & \cdots 98 & 98 & 99 \\ 2 & 3 & \cdots & 100 & 3 & 4 & \cdots 99 & 100 & 100 \end{pmatrix} \quad (8)$$

Based on the ANOVA theory and the form of Eq. (6) and Eq. (7), the ANOVA model can be expressed as Eq. (9). It is composed by the mean effects of SWAT model parameters (α_h), GCMs model (β_k), emission scenarios (γ_l), internal variability($\eta_{h,j,l}$) and interaction effects ($\xi_{h,j,l}$). The mean effects can be computer as the deviation of each factors mean value and the global mean $M^{g(-,j),-,-}$.

$$M^{g(h,j),k,l} - M^{g(-,j),-,-} = \alpha_h + \beta_j + \gamma_l + \eta_{h,j,l} + \xi_{h,j,l} \quad (9)$$

In the ANOVA model, the total variance of the hydrological variable $M^{g(h,j),k,l}$ is expressed as the total sum of squares (SST), and it can decompose into individual variance of each effect:

$$SST = SSA + SSB + SSC + SSIV + SSI \quad (10)$$

Where SSA, SSB, SSC is the uncertainty contribution of SWAT model parameters, GCMs, emission scenarios respectively, SSIV is the internal variability and SSI is the contribution of the interaction effects between SWAT model parameters, GCMs and emission scenarios.

By this approach, the intercomparisons among the uncertainty contribution of SWAT model parameter, GCMs, emission scenarios, internal variability and the interaction effects are not affected by the different sampling number.

4 Results

4.1 Hydrological model parameters calibrated and uncertainty

The SWAT model is constructed based on the historical daily meteorological data and spatial geographic data of the study basin. Before being used to predict the future runoff, the hydrological model parameters need to be calibrated and validated. This study divided the calibration period (1982~1996) and validation period (1997~2011) based on the precipitation and runoff changing trends. The simulated data from the SWAT was compared with the historical observed data to ensure its reliability. Three metrics E_{NS}, R_e, and R^2 are been used to estimate the model performance during calibrated and validated period. More details about the calibration and validation were introduced in (Zhu et al. 2018). The SUFI2 method is used to calibrate the parameters for the 1982-2011 period runoff in study area. The parameters setting was shown in

282 Table 2.

283

284 Table 2 The selected SWAT model parameters

Parameter	Definition	Min	Max
CN2	Initial SCS runoff curve number for moisture condition	0.75	1.25
SURLAG	Surface runoff lag coefficient	1.00	23.98
LAT_TTIME	Lateral flow converge coefficient	0.01	179.92
ESCO	Soil evaporation compensation factor	0.01	1.00
GW_DELAY	The delay time	0.37	500.00
ALPHA_BF	Baseflow alpha factors (days)	0.00	1.00
GWQMN	Threshold depth of water in the shallow aquifer required for return flow to occur	0.41	499.72
SFTMP	Snowfall temperature	-5.00	5.00
SMFMX	Melt factor for snow	1.50	8.00
TIMP	Snowmelt temperature lag factor	0.01	1.00

285

286 The SUFI2 is used as a parameter uncertainty estimate method for reference period in the study
287 basin. For final ensemble of the 100 parameter sets generate by the LHS, and then these parameter
288 sets are put in the SWAT model to generate 100 behavioral simulations which are performance in
289 Fig. 3 with the help of box plots. Each box represents 100 behavioral simulations which outputs
290 by the calibrated SWAT model. The length of the box plots denotes the runoff changes range from
291 100 simulations corresponding to one specific month. The differences between two boxes shows
292 the parameters effect are quite differently for one given month. It can be seen in Fig. 3 that the
293 month runoff change range due to SWAT model parameter sets are relatively larger in June to
294 September. As the June to September is the flooding season of the watershed, the uncertainty of
295 runoff may play important role in flood control and management. Hence, the uncertainty
296 contribution of the SWAT model parameter sets need be quantified.

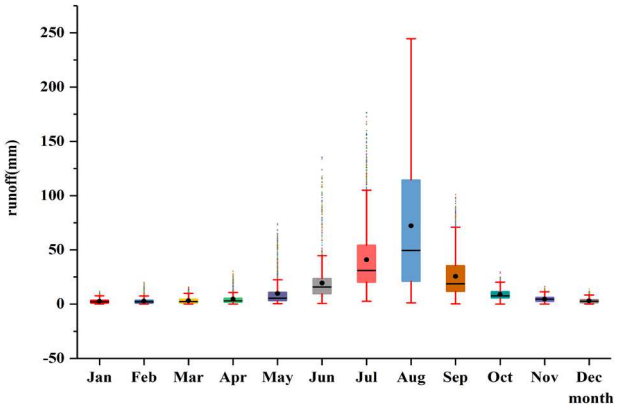

297

298 Fig.3. The SWAT model parameters uncertainty of the reference periods.

299

300 **4.2 Estimating the uncertainties of hydrological climate-impact projections**
301 **under climate change**

302 **4.2.1 Changes in precipitation projections**

303 The precipitation projections in 2050s and 2080s are compared with the reference period and
304 demonstrated in Fig.4. It can be seen that the lots of scenario members performance a marked
305 increase trend in 2050s and 2080s, however, several members show a decreased trend.

306 Take 2050s summer for example, all of the precipitation projections show an increased trend
307 except for CMCC-CM and MPI-ESM-MR performance an decreased trend under RCP8.5
308 scenarios, the precipitation changing interval is from 54.13% increase to -21.2% decrease. The
309 uncertainty of precipitation projections is significant in the 2080s winter, which changes from
310 -19.79% to 95.95%. In contrast, the changing rang of spring and autumn are relatively small,
311 among the two future periods, the uncertainty range of spring is from 31.2% to -21.27% in 2050s,
312 and the range from 1.71% to 41.18% in 2080s autumn. Compared to the other seasons, the change
313 range of spring is smallest in 2080s.

314 The precipitation projections of different GCMs in the same emission scenarios and periods
315 displays a obvious changing range. It can be noted that the precipitation projections have
316 non-negligible uncertainty in future. This uncertainty of precipitation propagates through the
317 hydrological model and is amplified in the runoff outputs. Hence, the precipitation uncertainty
318 under climate change need be investigated previously.

319

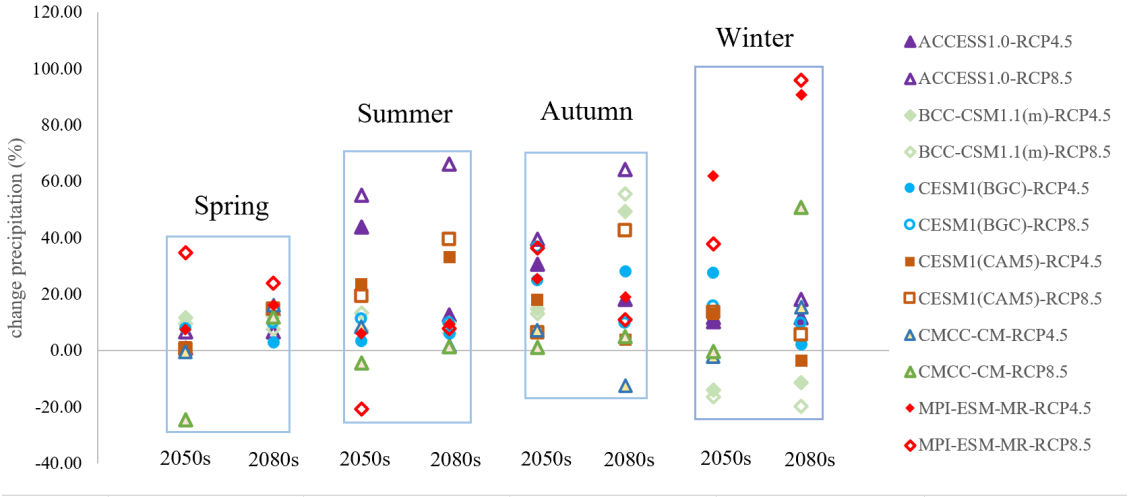

Fig.4. The uncertainty range of the precipitation change is shown for the four seasons.

4.2.2 Change in temperature projections

The box chart of Fig.5a and Fig.5b shows the maximum and minimum temperature projections (T_{max} and T_{min}) compared to the reference period, the temperature projections show a univocal increased trend for each scenarios member. Specifically, in the 2050s period, the mean temperature increases of 1.95 ℃ under RCP4.5 and 2.73℃ under RCP8.5, while increase of 2.73 ℃ under RCP4.5 and 4.20℃ under RCP8.5 in the 2080s period. Moreover, the increase ranges of the T_{max} are larger in summer and autumn than the other season. The summer mean of T_{max} increases by 1.84℃ and 2.52℃ in two future periods under RCP4.5. Again, the increase range of T_{max} also significant under RCP8.5, where the increase of mean T_{max} were 2.61℃ in 2050s summer and 4.17℃ in 2080s autumn. The changing trend of T_{min} shows a similar increasing trend in two future periods, and the ranges of increase of mean T_{min} are all above 4.0℃ in summer, autumn and winter under RCP8.5.

From the T_{max} and T_{min} changing result in 2050s and 2080s under two emission scenarios, it can be found that the increase temperature became larger as the time increased into future period, and increased range is larger under RCP8.5 than RCP4.5. It can be also obtained that the uncertainty of temperature is marked in future among different scenario members, the mainly uncertainties source need be quantified and estimated.

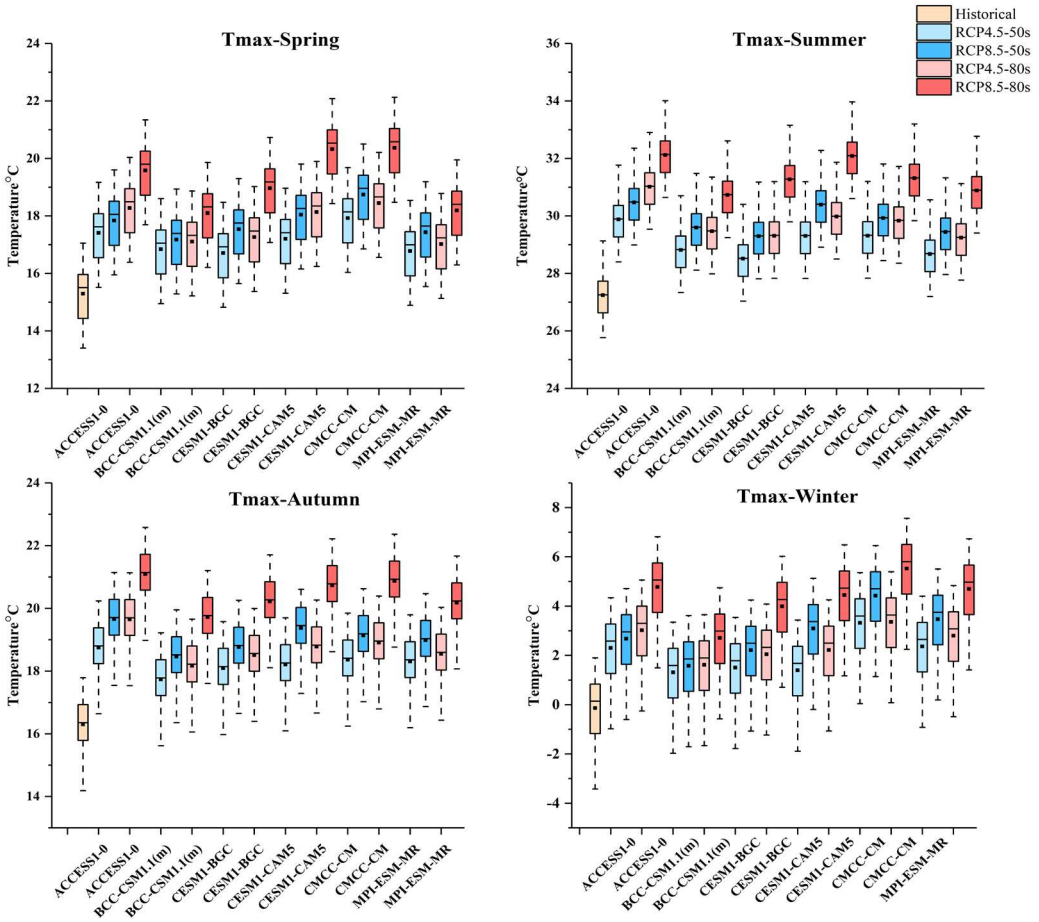

Fig.5a The Tmax in 2050s and 2080s under RCP4.5 and RCP8.5 scenarios based on 6 GCMs compare with reference period (1980-2004). Lower and upper box boundaries indicate the 25th and 75th percentiles, respectively. The black lines and dots inside the box represent the median and mean value, respectively. The lower and upper whiskers indicate the 10th and 90th percentiles, respectively.

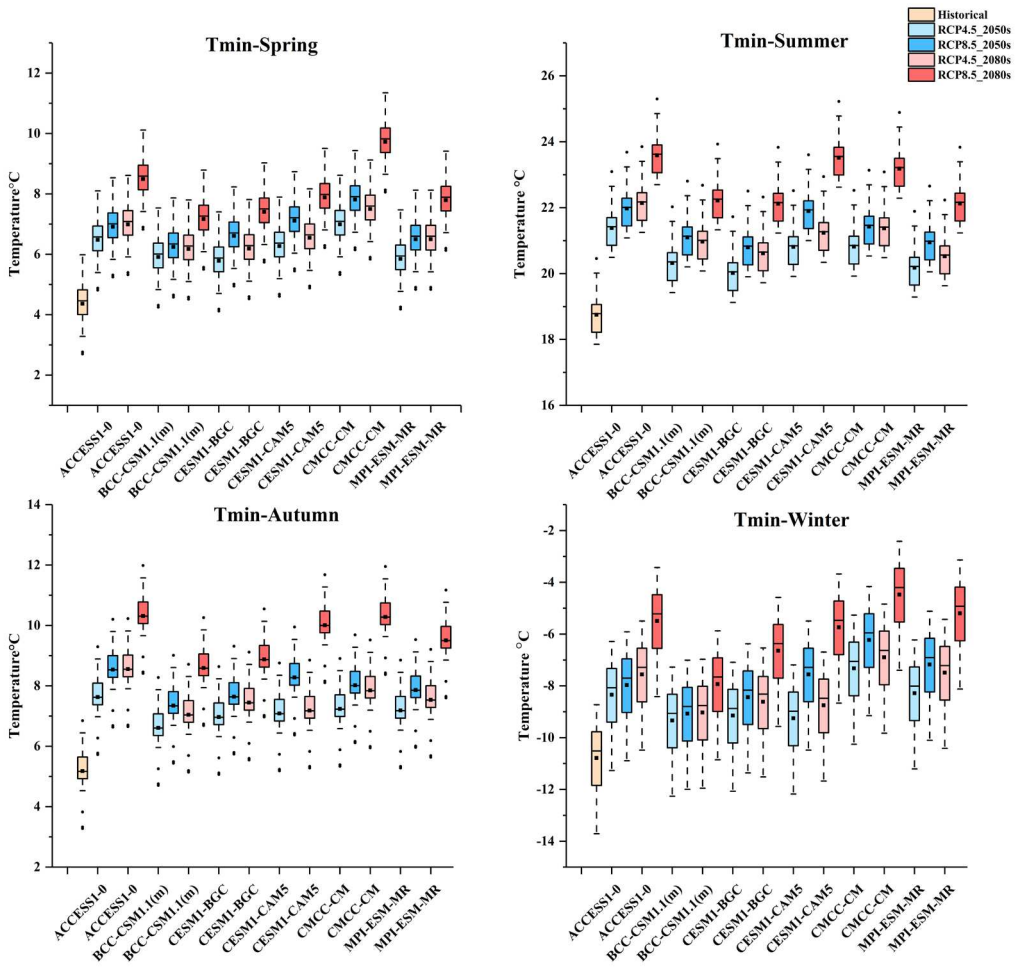

Fig.5b The T-min in 2050s and 2080s under RCP4.5 and RCP8.5 scenarios based on 6 GCMs compare with reference period (1980-2004). Lower and upper box boundaries indicate the 25th and 75th percentiles, respectively. The black lines and dots inside the box represent the median and mean value, respectively. The lower and upper whiskers indicate the 10th and 90th percentiles, respectively.

4.2.3 Change in ET projections

The calibrated hydrological model output 100 behavioral simulations for each scenarios member in each month. There are 1200 sets ET projections can be obtained from the hydrological simulation for two future periods, and the future season ET projections comparing with baseline period shows in Fig.6a and Fig.6b. For RCP4.5 and RCP8.5 emission scenarios, the season mean ET projections shows an obvious increased trend in spring, summer and winter. However, the mean ET of autumn demonstrate a relatively smaller increased, some of the models show a decreased trend. In contrast with precipitation and temperature projections, the various of ET projections among each scenarios members are relatively smaller.

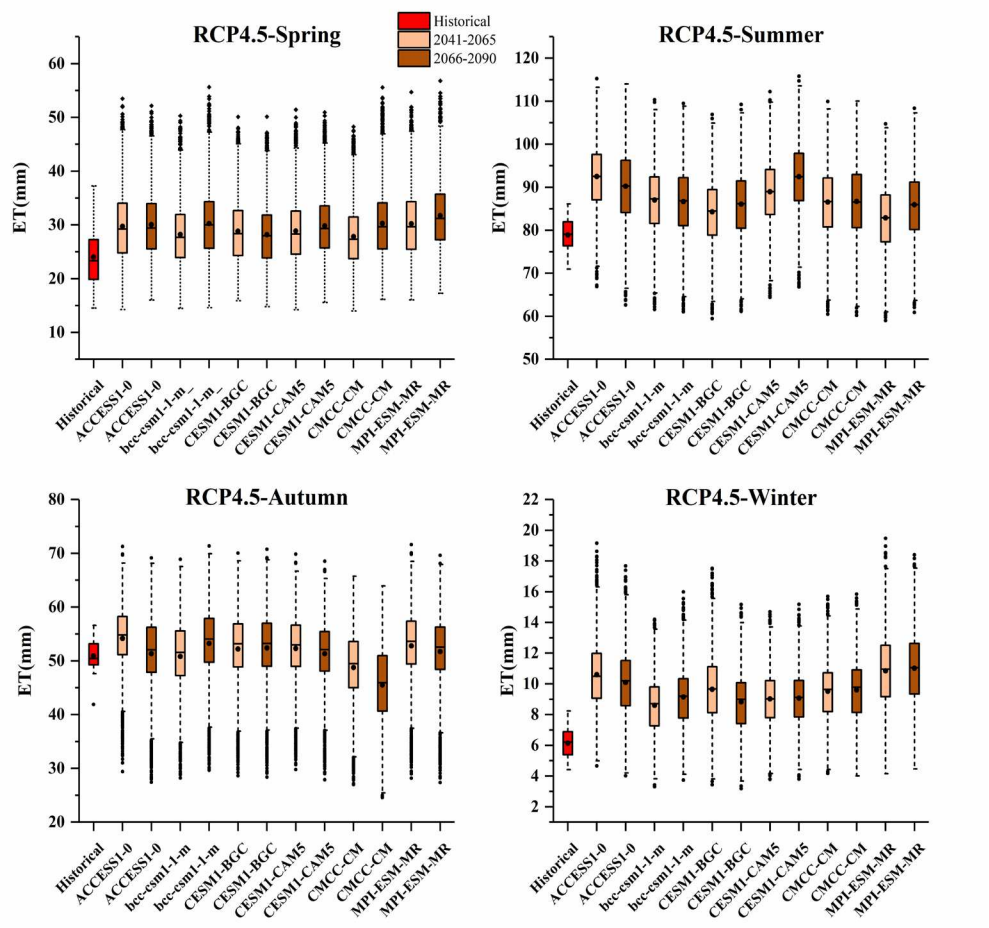

362

363 Fig.6a The ET in 2050s and 2080s under RCP4.5 scenarios based on 6 GCMs compare with
364 reference period (1980-2004). Lower and upper box boundaries indicate the 25th and 75th
365 percentiles, respectively. The black lines and dots inside the box represent the median and mean
366 value, respectively. The lower and upper whiskers indicate the 10th and 90th percentiles,
367 respectively.

368

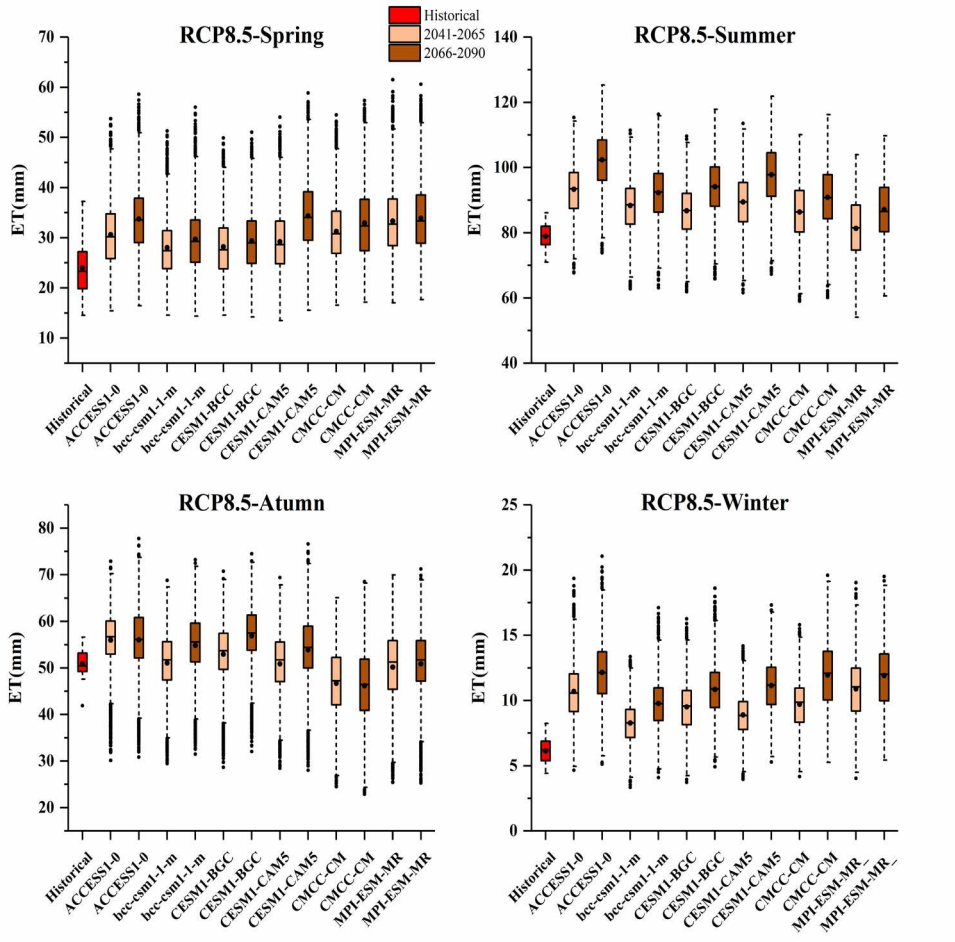

Fig.6b The ET in 2050s and 2080s under RCP8.5 scenarios based on 6 GCMs compare with reference period (1980-2004). Lower and upper box boundaries indicate the 25th and 75th percentiles, respectively. The black lines and dots inside the box represent the median and mean value, respectively. The lower and upper whiskers indicate the 10th and 90th percentiles, respectively.

4.2.4 Change in runoff projections

The predicted runoff projections of four seasons in two future periods are compared with the reference period in Fig.7a and Fig.7b, each box and whisker plots for runoff projections are generated from 1200 simulation chains. For 2050s, the runoff projections increase more significant in autumn than the other seasons. In terms of autumn runoff changing, lots of scenarios members show an increased trend in future, ranging 1.37% ~66.01 % under RCP4.5 and -11.99 % ~97.08 % under RCP8.5. In comparison with autumn runoff, the runoff projections in summer trending a relatively small decreased in future. The range of runoff changing is from -18.41% to 47.78% under RCP4.5 in 2050s, there are four scenarios member demonstrate an decreased trend such as BCC-CSM1.1(m) (-13.70), CESM1-BGC (-18.41), CMCC-CM (-11.81), MPI-ESM-MR (-13.97). The range of runoff changing is from -52.78% to 70.41% under RCP8.5 in 2050s, it can

be found that the diversity of runoff is larger in this scenarios and most of scenarios members shows an decreased trend in future. For 2080s, the obvious changing of runoff is summer and autumn. Most of scenarios members show an increased trend in autumn runoff, the mean changing ratio is 33.89% under RCP4.5. In contrast with autumn runoff, the runoff changing in summer show a decreased trend, and the mean changing ratio is -8.56% under RCP4.5. Similarly, the runoff projections still exist obvious differences among scenarios members. The changing trend of runoff projections demonstrated a consistent increased trend under RCP8.5, the mean changing ratios of spring, summer, autumn and winter is 2.91%, 11.95%, 85.22% and 25.68% respectively. Furthermore, the diversity of runoff projection still significantly in 2080s under RCP8.5 scenarios.

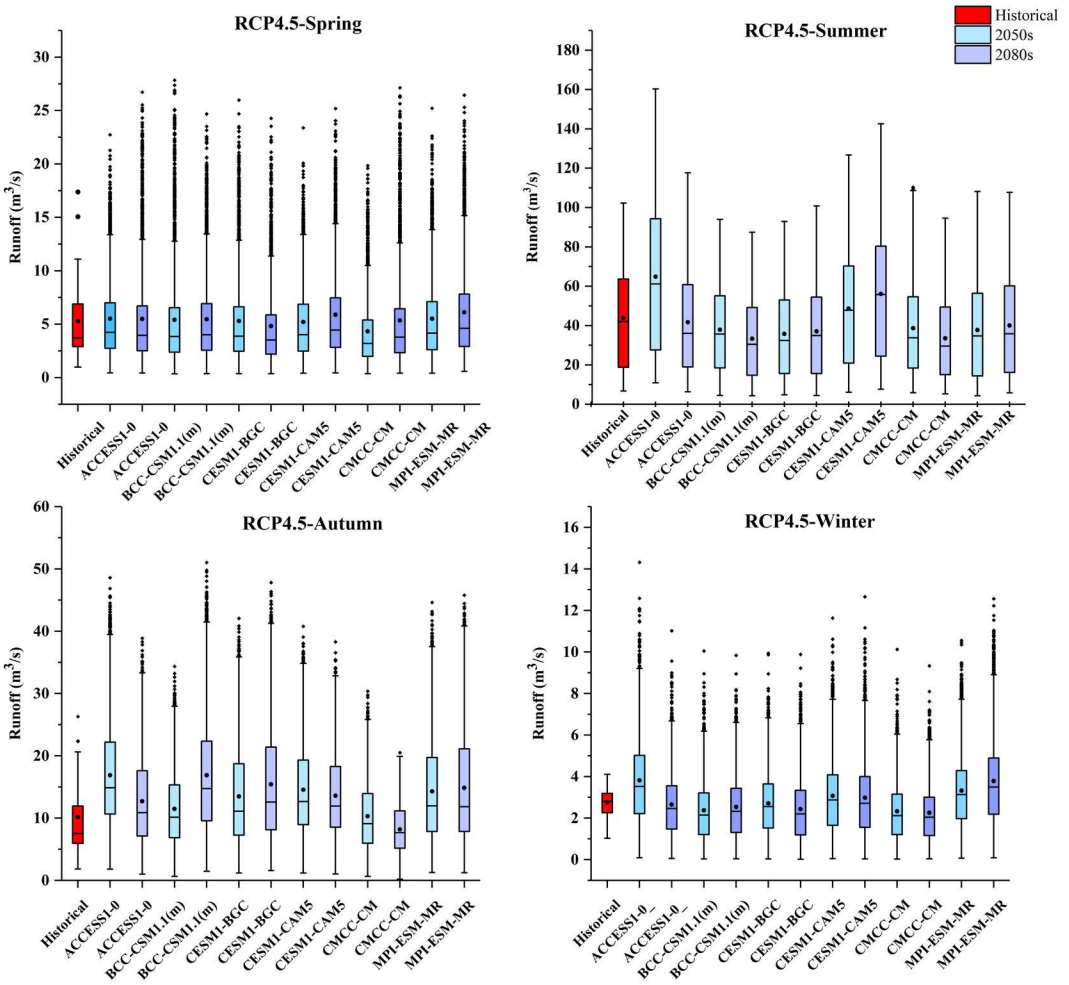

Fig.7a The runoff in 2050s and 2080s under RCP4.5 scenario based on 6 GCMs compare with reference period (1980-2004). Lower and upper box boundaries indicate the 25th and 75th percentiles, respectively. The black lines and dots inside the box represent the median and mean value, respectively. The lower and upper whiskers indicate the 10th and 90th percentiles, respectively.

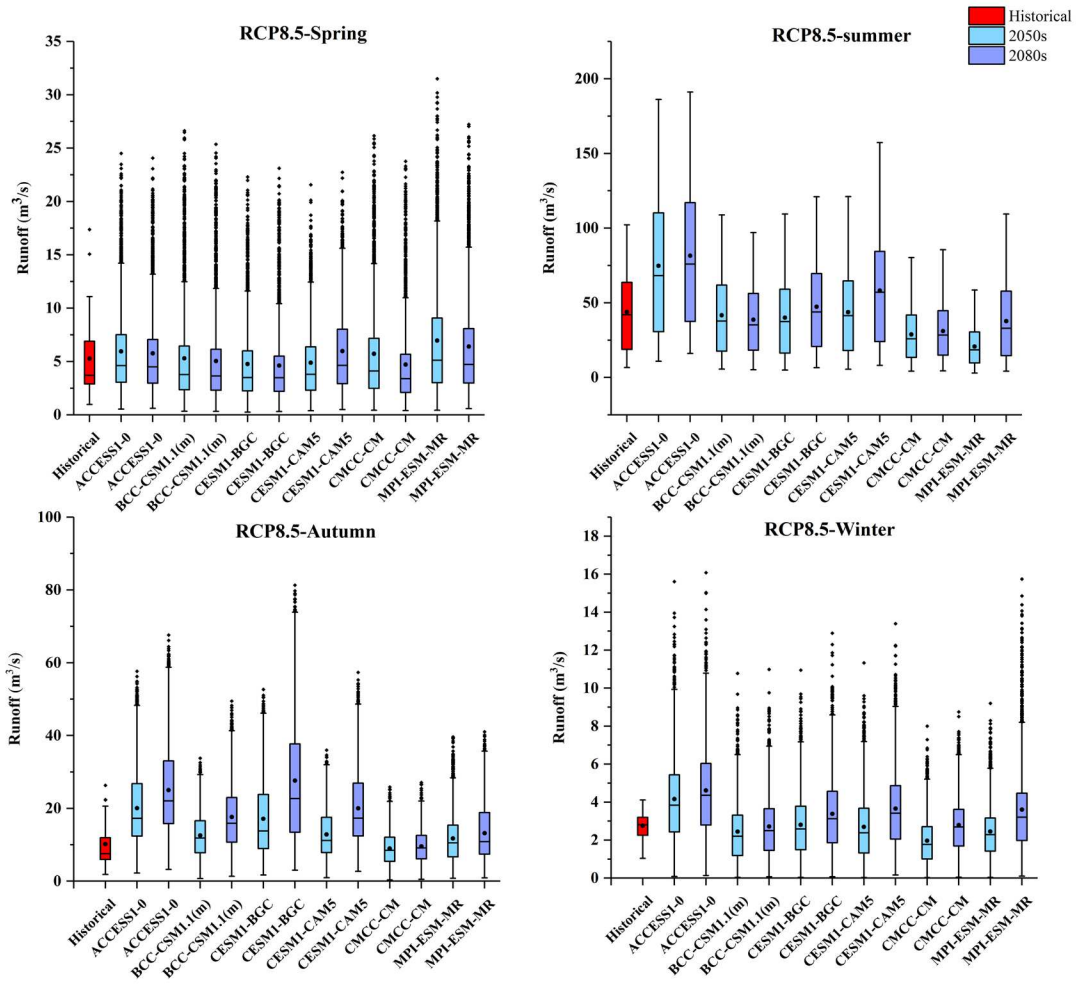

Fig.7b The runoff in 2050s and 2080s under RCP8.5 scenario based on 6 GCMs compare with reference period (1980~2004). Lower and upper box boundaries indicate the 25th and 75th percentiles, respectively. The black lines and dots inside the box represent the median and mean value, respectively. The lower and upper whiskers indicate the 10th and 90th percentiles, respectively.

Furthermore, the box-and-whisker plots show in Fig.7a and Fig.7b, the upper and lower ends represent the highest and lowest runoff, and the change range indicated the uncertainty bound. Compared with the runoff in reference period, the autumn runoff projections reveal a consistent increase in mean and median values under both two emission scenarios and future periods. Most of the summer runoff projections show a decrease trend in future. From the runoff projections changing results, each scenarios member demonstrated a wide uncertainty range inner member, and a obvious diversity among different members. Accordingly, the uncertainty ranges of runoff projections under RCP8.5 projections are larger than RCP4.5 scenarios. Compared with the other seasons, the summer runoff projections showed the largest uncertainty brands under two emission scenarios in future. Observing median values, the summer and autumn projections in 2050s and

418 2080s show the non-negligible differences, for example, the median values for summer under
419 RCP4.5 scenario feature a decrease in projections as BCC-CSM1.1(m), CESM1-BGC,
420 CMCC-CM and MPI-ESM-MR, which ranging from -22.82% to -15.04%, in contrast, the median
421 values show an increase from 45.55% to 13.79% in projected of ACCESS1 and CESM1-CAM5.
422 In addition, the median values for the spring runoff projections in 2050s under RCP4.5 portray a
423 consistent slight increase from 3.23% to 12.51%, only CMCC-CM projection show a decrease as
424 -12%. Overall, the runoff projected by all GCMs showed a large uncertainty in two future periods.
425 Comparing 2050s and 2080s, it can be found that the lower ends become smaller and the upper
426 ends become larger, which indicate that the uncertainty bonds increasing from 2050s to 2080s. In
427 addition, comparing the RCP4.5 and RCP8.5 scenarios, the uncertainty bound of RCP8.5
428 scenarios are always larger than RCP4.5.

429 **4.2.5 Impacts of climate factors to runoff change**

430 After analyzing the changes of climate factors (precipitation, T_{max}, T_{min} and ET) in future, it can
431 be found that the different climate factors performance different changing trend and uncertainties
432 under climate changing. The different climate factors may effect and produce different uncertainty
433 contribution to runoff changing, hence, it is important to analyze the relationship between climate
434 factors and runoff projections. In order to determine the relationships between them, the multiple
435 linear regression was performed for each model chain using changes of precipitation, T_{max}, T_{min}
436 and ET as the independent variables and the runoff as the dependent variables.

437 The regression coefficients for runoff are shown in Table 3. In general, the increase of
438 precipitation may cause a positive effect on runoff increasing, this trend can be found in all of the
439 models and scenarios and coefficients at the 0.001 significant level. In contrast, the increase of ET
440 projections was negatively related to runoff, and there are seven projections at the 0.001
441 significant level. In addition, the increase T_{max} and T_{min} may contribute the increase trend of runoff,
442 however, the coefficients did not pass the significant test even at 0.05 level. In most scenarios
443 members, the precipitation and ET had a significant influence in runoff projection and temperature
444 had a slight influence, hence, the internal variability of climate factor need be investigate
445 specifically.
446
447
448

Table 3 The multiple liner regression coefficients for runoff (R mm year^{-1}) with maximum temperature (T_{max}℃), minimum temperature (T_{min}℃), precipitation (P mm year^{-1}) and ET (mm year^{-1}) in a multiple linear regression model ($R= a_1 T_{max}+ b_1 T_{min}+ c_1 P+ d_1 ET+ e_1$). p is the significant level：***: p<0.001, **: p<0.01, *: p<0.05.

Models	a_1	b_1	c_1	d_1	e_1	R^2
ACCESS1-0_RCP45	22.75	-21.40	0.92***	-0.97***	-197.62**	0.96
ACCESS1-0_RCP85	61.05	23.89	0.97***	-0.86	-1284.58	0.75
BCC-CSM1.1(m)_RCP45	20.96	-15.30	0.85***	-0.81***	-237.05	0.92
BCC-CSM1.1(m)_RCP85	17.26	-13.92	0.84***	-0.76**	-205.54	0.93
CESM1(BGC)_RCP45	28.98	-25.77	0.86***	0.21***	-209.88	0.93
CESM1(BGC)_RCP85	81.42	-38.46	0.99***	-0.5	-1370.22***	0.86
CESM1(CAM5)_RCP45	18.15	-17.34	0.90***	-0.93	-153.06	0.96
CESM1(CAM5)_RCP85	22.13	-20.34	0.87***	-0.77***	-265.73	0.96
CMCC-CM_RCP45	5.92	18.26	0.62***	-0.53	-248.50	0.75
CMCC-CM_RCP85	15.40	-14.67	0.68***	-0.45*	-235.24	0.87
MPI-ESM-MR_RCP45	29.52	-24.95	0.88***	-1.02***	-224.86	0.94
MPI-ESM-MR_RCP85	24.93	-15.04	0.77***	-0.65**	-348.45	0.90

4.3 Evaluation and investigation the source of uncertainty

4.3.1 Estimating the role of internal variability

The role of internal variability in hydrological climate-impact projections is partitioned and quantified in this section. In order to investigate the internal variability of the precipitation trends, six GCMs are forced by the same emission scenarios, and then the CIV values of the hydrological climate-impact projections under two emission scenarios were shown in Fig.8.

The CIV values of precipitation are higher in rainy season (June to September) and the lowest values appeared in winter. It is demonstrated that the internal variability play an important role on the uncertainty of flood season precipitation. Similarly, the CIV values of ET are larger in May to September than the other months. In contrast, the CIV values of T_{max} and T_{min} are relatively smaller in rainy season. Moreover, the CIV values of runoff demonstrate that the internal variability is higher in rainy season than the other seasons, these trend is similarly with the CIV of precipitation and ET projections. According to the multiple linear regression of the climate factors, the precipitation and ET have significant influence on runoff, it can imply that the internal variability of precipitation and ET may influence the internal variability of runoff.

From the CIV values of runoff projections under RCP4.5 and RCP8.5 emission scenarios, it can be found that the CIV values of rainy season are larger than the other seasons, and the maximum CIV value of the runoff projections appeared in August. Compared the CIV values of precipitation,

471 temperature, ET and runoff projections, the internal variability of precipitation and runoff showed
472 obvious increased in rainy season. On consideration of the internal variability may combine with
473 the model and scenarios uncertainties and then influencing the runoff, hence, the contribution of
474 internal variability need be special investigated.

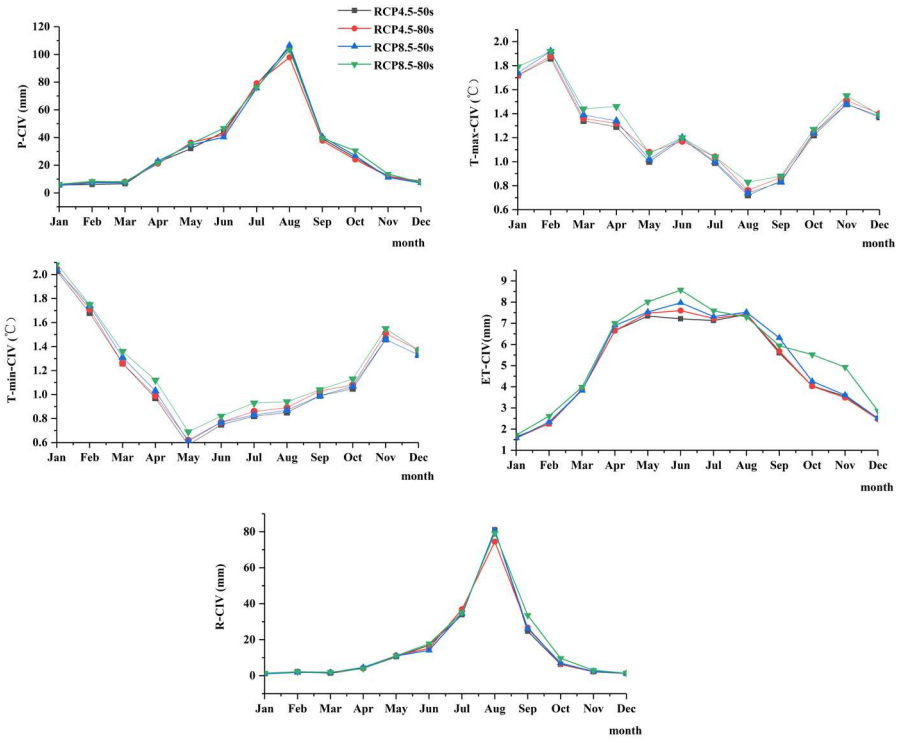

475

476 Fig.8. The CIV values of hydrological climate-impact projections

477 The SNR can give some useful information for investigating the role of internal variability. The
478 SNR values of precipitation, temperature, ET and runoff are showed in Fig.9. This metrics convey
479 information about the magnitudes of the forced and internally generated components of
480 hydrological climate-impact projections under future climate change. The SNR of ET and
481 temperature show an obvious changing in spring, summer and autumn.The SNR values of T_{max}
482 and T_{min} demonstrated a relatively higher values in June to October, it worth noting that the
483 external forcing is the mainly impact factors in these month. Similarly, the SNR of ET is higher in
484 June to October than the other month, hence, the internal variability of temperature and ET is
485 weaker in these season. In contrast, the SNR of precipitation and runoff are relatively stable
486 among four seasons. An important result is that the internal variability contributed a considerable
487 higher component in precipitation and runoff than temperature and ET. On the base of the
488 estimating of internal variability, it can be observed that the SNR values of the precipitation and

runoff mostly around 1 in each month. It means the significance of internal variability is approximate with external forcing. However, the SNR values can't able to quantify the internal variability. It is important to partition and confirm the specific internal variability and other uncertainty source contribution inner year.

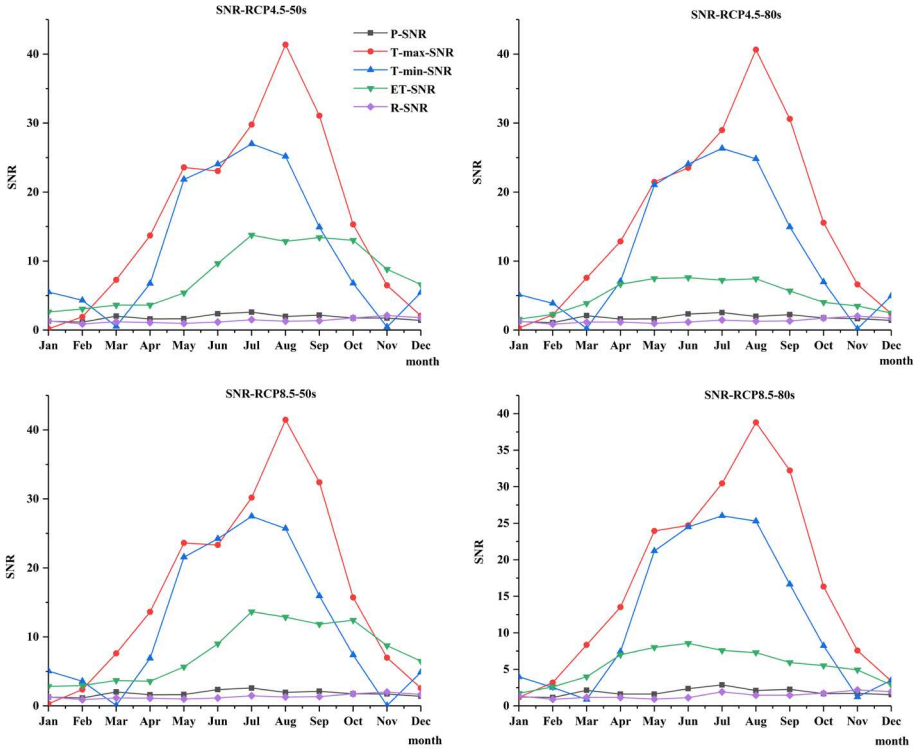

Fig.9 The SNR values of hydrological climate-impact projections

4.3.2 Contribution analysis of uncertainty sources

As mentioned previously, the uncertainty sources of hydrological climate-impact projections involve model uncertainty, scenarios uncertainty and internal variability. The ANOVA method is used to quantified the uncertainty contribution of different sources of uncertainty in 2050s and 2080s.

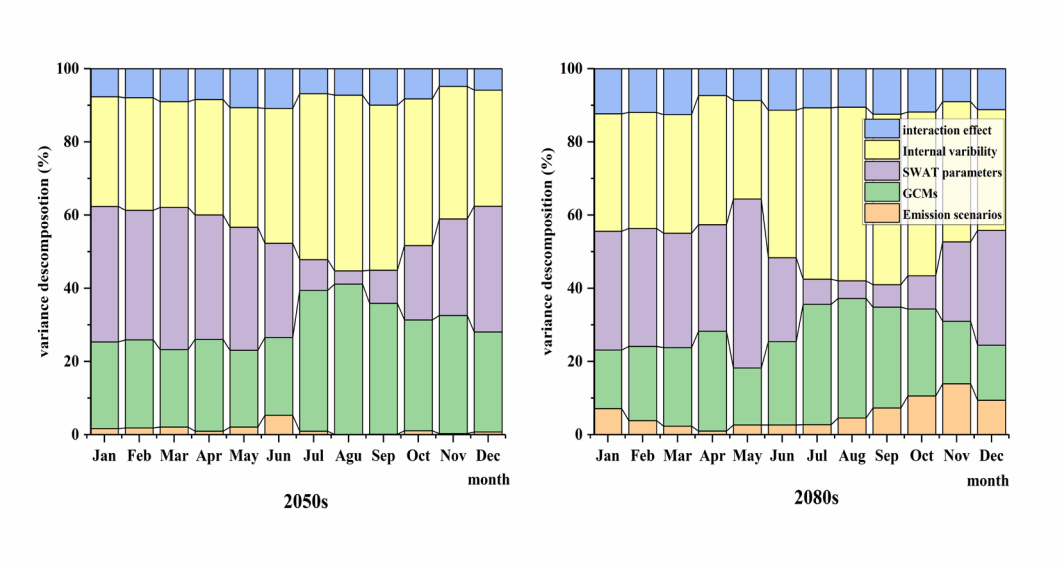

Fig.10 The contribution of uncertainty sources to the runoff in 2050s and 2080s period.

The contribution of uncertainty sources showed in Fig.10. It is noteworthy that the effect of internal variability is significant among all of the month in 2050s and 2080s period. The contribution of internal variability is almost equal with the sum of the uncertainty of GCMs and emission scenarios. It contributes 29% ~ 48% and 31.4% ~ 47.4% of the total variance in 2050s and 2080s, respectively. Moreover, the biggest contribution embodies in September in two future periods. The other two mainly uncertainty contributors are GCMs and SWAT model parameter sets. The uncertainty of GCMs account for 21% ~ 41% and 15% ~ 33% in 2050s and 2080s, and the biggest value is in September (2050s) and August (2080s) respectively. For the SWAT model parameter sets, the contribution accounts for 4% ~ 39% and 4.8% ~ 32.4% in 2050s and 2080s, respectively. Compared with the previous two uncertainty sources, the SWAT model parameters main effect the Spring (March to May) and Winter (December to February) runoff projections. The interaction term contribution to the runoff projection explaining approximately 8% ~ 11% and 7% ~ 12% throughout the 2050s and 2080s periods, respectively. The contribution of emission scenarios is relatively small, which bellows 5% and 10.5% in 2050s and 2080s, respectively.

Overall, the results of uncertainty decomposition in Fig. 10 indicate that internal variability and GCMs are dominant uncertainty contributor of runoff in June to October. In addition, SWAT model parameters are the mainly uncertainty contributor in spring and winter. In summary, the internal variability and GCMs provide mainly uncertainty contribution in summer and early autumn, and the mainly uncertainty contributor of runoff in spring and winter are internal variability and SWAT model parameters.

5 Discussion

5.1 Hydrological cliamte-impact projections changing

This study estimated hydrological climate-impact projections changes under climate change impacts in a respective watershed in Northeastern China. Compared with the reference period, the temperature and precipitation projections performance an increased trend in two future periods, and this increased trend is more significant under RCP8.5 emission scenarios and later future period as 2080s. This finding is consistence with some previous publications, Wang et al. (2020) found that the response of hydrological extreme events to climate changing shows much higher in 2070-2099 under RCP8.5 scenarios. In addition, the ET projections shows obvious increase trend in summer and winter, and a relatively small increase trend in autumn. It can be found that the runoff projections show an increased trend in autumn and a slight decreased trend in summer. With the combined influence of increasing precipitation, temperature and ET in summer, there is a high possibility that runoff would decrease in summer. In contrast, a relative sightly increase of ET in autumn may due to run off increase. Since precipitation, temperature and ET are important input to hydrological model, thus the uncertainties of these projections may also influence runoff projections. Moreover, through the multiple linear regression analysis, the precipitation and T_{max} had a significant positive effect on runoff, ET and T_{min} shows a relatively small negative effect on runoff. Hence, the increase precipitation and relatively small increase ET may due to a relatively obvious increased in autumn.

This manuscript also found the predication of both hydrological climate-impact projections showed wider range under RCP8.5 than RCP4.5, especially in 2080s. Moreover, the projected of runoff in future also demonstrated an obvious diversity in future, especially in Summer and Autumn. To deal with the uncertainty in future runoff, the details of sources of uncertainties need to be investigated and quantified, so that a relatively reliable hydrological projections are produced.

5.2 The role of internal variability

Since the internal variability plays an important role in the uncertainties of the hydrologial climate-impact projections, thus the CIV of future projections has been investigated under RCP4.5 and RCP8.5. The findings indicated that the internal variability of precipitation, ET and runoff are larger in June and September than the other month. In order to investigate the magnitudes of the

552 external forcing and internal variability, the SNR of future projections has been investigated under
553 RCP4.5 and RCP8.5. The SNR values of precipitation and runoff are stable, the values are all
554 around 1 among 12 months, which means that the internal variability and external forcing
555 performance an equality effect. However, it is difficult to determine which is the important
556 influence source of hydrologial climate-impact projections only by the SNR values. Considering
557 the June to September contains the entirely flood season in research watershed, the annual internal
558 variability and external forcing uncertainty contribution of runoff projections need be investigated
559 particularly.

560 **5.3 Estimating the source of uncertainties**

561 The ANOVA framework was constructed to quantify the uncertainty sources contribute to the
562 overall uncertainty, furthermore, in considering the substantial effects of internal variability on the
563 uncertainty of runoff projections, the uncertainty contribution of internal variability has been
564 considered to ensure the comprehensive of uncertainty assessment.

565 Quantifying the source of uncertainties contribution to future runoff projections can provide
566 insights into finding the mainly effect factors of runoff variety under climate changing. On the
567 base of the SNR values of different projections, the internal variability and external forcing of
568 precipitation and runoff shown equally significance, which can be embodied in uncertainty
569 estimating. In rainy season (June to September), the internal variability and GCMs are the mainly
570 uncertainty contributors in runoff projections. In contrast, the internal variability and SWAT model
571 parameter sets provided obvious uncertainty to runoff in January to May and October to
572 December.

573 These findings indicate that the internal variability is the important uncertainty sources among
574 the different sources chosen by this study, which agree with the findings of some previous
575 publications (Lafaysse et al. 2014; Hingray et al. 2019). Meanwhile, the runoff projections are
576 significantly impact by the choices of GCMs, this point also has been found in many studies
577 (Kujawa et al. 2020), for instance, Zhang et al. (2021) found the disparity between different
578 GCMs may mainly impacted the climate change researches, and the increased sample sized of
579 GCMs may conduct a complete uncertainty assessment. As an important tool for runoff simulation
580 and prediction, the hydrological model is a non-negligible uncertainty contributor of overall
581 uncertainty, among the uncertainty derive form the hydrological model, the model parameters

582 obtained more attention (Keller et al. 2019; Vaghefi et al. 2019; Nerantzaki et al. 2020). Moreover,
583 the contribution of and interaction effect are relatively small compared with the other uncertainty
584 sources, these findings consist with some previous researches (Bosshard et al. 2013; Qi et al. 2016;
585 Vaghef et al. 2019).

586 The quantifying of internal viability has been demonstrated in several previous studies
587 (Lafaysse et al. 2014; Evin et al. 2019; Hingray et al. 2019), however, most of the studies focused
588 on decomposition the internal uncertainty of climate system through hydrological simulation
589 process (Doi and Kim. 2020; Yu et al. 2020; Maher et al. 2020; Hawkins and Sutton. 2011).
590 Moreover, this study indicates that the internal variability, GCMs model, emission scenarios,
591 hydrological model parameters and interaction effects need be quantified entirely. Because of the
592 annual distribution contribution of different sources are the important information of uncertainty
593 analysis. The contribution of uncertainty sources in each month can be found in the uncertainty
594 quantified results straightforward.

595 On consideration of the internal variability may propagate in the hydrological simulation
596 process and then effected the runoff uncertainty. Quantifying the internal variability of
597 precipitation, temperature and ET can provide some useful information to runoff uncertainty
598 analysis. For rainy season, the internal variability and GCMs are the dominant uncertainty in
599 runoff. On the base of multiple linear regression, the precipitation and ET has significantly
600 influence on runoff, and their uncertainty can also influence on runoff uncertainty. From the CIV
601 and SNR values of climate projections, it can be found that the internal variability of precipitation
602 and ET are large in rainy season. Hence, the internal variability of precipitation and ET may affect
603 runoff to some extent. Above all, the internal variability obvious role of the in shaping overall
604 uncertainty, and some of the uncertainty source of runoff projections can be trace bake to
605 precipitation and ET etc.

606 ## 6 Conclusion

607 The details of sources of uncertainty in hydrological climate-impact projections has been
608 investigated and quantified in this manuscript. The uncertainty quantifying and estimating are
609 essential for the runoff prediction. In addition, identifying the fundamental uncertainty source is
610 meaningful to reduce existing uncertainties in future. The main conclusions of this study can be
611 summarized as flowing:

(1) Based this study analysis of future climate conditions for the Biliu River basin, it can be found that the precipitation and temperature shown an increasing trend in future, especially in RCP8.5 and later future period. In addition, the climate factors may produce different influence and uncertainty contribution to runoff changing. For instance, the precipitation has a significant positive effect on runoff and ET shows a relatively small negative effect. Hence, the changing of precipitation and ET may due to corresponding changing in runoff. Furthermore, the wide uncertainty ranges can be found in each projections, the sources of uncertainty may obvious influenced the reliable of hydrological process simulation in future.

(2) By elucidating the impact of climate internal variability of runoff projections, this study analysis the role of internal variability of hydrological climate-impact projections and find out the important influence factor of uncertainty of runoff projections. In term of precipitation and ET, the internal variability is larger in June to September, and the SNR values also shows the internal variability and external forcing are both important influence factors to runoff. Combining with the internal variability and GCMs are the dominate uncertainty contributors in June to September. It is worth noting that the internal variability can propagate in the hydrological simulation process, and the internal variability of runoff projections is remarkable in flood season of study watershed in future. As the rain season in the study basin, some water resources adaptation measures need be planned to alleviate the climate change influence, especially in high emission scenarios (RCP8.5) and far future (2080s).

(3) The uncertainty contribution of internal variability with GCMs and SWAT model parameters are temporal variability. The internal variability and GCMs are the mainly uncertainty contributors OF runoff projections,IN rainy season (June to September). In contrast, the internal variability and SWAT model parameter sets provided obvious uncertainty to runoff in January to May and October to December. The findings of this study indicate that the role of internal variability of hydrological climate-impact projections is noticeable in future, these kinds of effect may extremely influence the stakeholders and local water resources government to provide correct hydrological regulation and flood control measures.

Funding Statement
This study was sponsored by the Open Research Fund of State Key Laboratory of Simulation and Regulation of Water Cycle in River Basin, China Institute of Water Resources and Hydropower Research, Grant NO. IWHR-SKL-202103. (Wenjun Cai)

Conflicts of interest/Competing interests
The authors declare that they have no known competing financial interests or personal relationships that could have appeared to influence the work reported in this paper.

Author's Contribution
Conceptualization, Xuehua Zhao and Jia Liu; Methodology, Wenjun Cai and Jia Liu; Formal Analysis, Wenjun Cai and Jia Liu; Writing Original Draft Preparation Wenjun Cai and Xueping Zhu; Writing—Review & Editing, Wenjun Cai and Jia Liu; Funding Acquisition, Wenjun Cai.

Availability of data and material
The climate data in 1901-2099 for RCP4.5 and RCP8.5 were downloaded from the National Climate Center (http://ncc.cma.gov.cn). The long-term experiment data of 1850-2100 for the chosen six climate models in CMIP5 were downloaded from the Program for Climate Model Diagnosis and Itercomparison (PCMDI, http://pcmdi3.llnl.gov/esgcet/). Yearly and monthly precipitation and runoff data in 1958-2011 were obtained from the Biliu River Reservoir administration. Month meteorological data were obtained from the China Meteorological Data Sharing Service System (http://cdc.cma.gov.cn/inex.jsp). The Digital Elevation Model (DEM) data (90×90m) were obtained from the CGIAR Consortium for Spatial Information (CGIAR-CSI) (http://srtm.csi.cgiar.org). Soil type and land use maps were obtained from the Data Center for Resources and Environmental Sciences, Chinese Academy of Sciences (http://www.resdc.cn/fist.asp).

Code availability
The calculate code of climate internal variability and ANOVA are according to the corresponding formulas, which has already described in this manuscript.

Ethics approval
ALL that data and analysis in this manuscript are ethics approval.

Consent to participate
This manuscript consent to participate.

Consent for publication
This manuscript consent to publication.

Acknowledgements
This study was sponsored by the Natural Science Foundation of Shanxi Province, China. Grant No.201901D111060 and the Open Research Fund of State Key Laboratory of Simulation and

687 Regulation of Water Cycle in River Basin, China Institute of Water Resources and Hydropower
688 Research, Grant NO. IWHR-SKL-202103. We would also like to acknowledge the World Climate
689 Research Programme's Working Group on Coupled Modeling, which is responsible for CMIP.
690
691
692 ## References:

693 Anjum M N, WahabA, Huggel C, Qamar M U, Hussain E, Ahmad S, Waheed A (2019) Simulation of the projected
694 climate change impacts on the river flow regimes under CMIP5 RCP scenarios in the westerlies dominated belt,
695 northern Pakistan. Atmospheric Research 227: 233-248. https://doi.org/10.1016/j.atmosres.2019.05.017
696 Abbaspour K C, Yang, Maximov I, Siber R, Bogner K, Mieleitner J, Zobrist J, Srinivasan R (2007) Modelling
697 hydrology and water quality in the pre-alpine/alpine Thur watershed using SWAT, Journal of Hydrology
698 333:413-430. https://doi:10.1016/j.jhydrol.2006.09.014
699 Abbaspour K C, Johnson C A, van Genuchten M T (2004) Estimating Uncertain Flow and Transport Parameters
700 Using a Sequential Uncertainty Fitting Procedure. Vadose Zone Journal 3:1340-1352. https://doi:10.2113/3.4.1340
701 Aryal A, Shrestha S, Babel M S (2017) Quantifying the sources of uncertainty in an ensemble of hydrological
702 climate-impact projections. Theoretical and Applied Climatology 135: 193-209.
703 https://doi.org/10.1007/s00704-017-2359-3
704 Byun, K, Chiu C M, Hamlet A F (2019) Effects of 21st century climate change on seasonal flow regimes and
705 hydrologic extremes over the Midwest and Great Lakes region of the US. Science of the Total Environment 650:
706 1261-1277. https://doi.org/10.1016/j.scitotenv.2018.09.063
707 Bosshard T, Carambia M, Goergen K, Kotlarski S, Krahe P, Zappa M, Schar C (2013) Quantifying uncertainty
708 sources in an ensemble of hydrological climate-impact projections. Water Resources Research 49:1523-1536.
709 https://doi:10.1029/2011WR011533
710 Belcher S E, Hacker J N, Powell D S (2005) Constructing design weather data for future climates. Building
711 Services Engineering Research and Technology 26: 49-61. https://doi.org/10.1191/0143624405bt112oa
712 Beven K, Binley A (1992) The future of distributed models: model calibration and uncertainty prediction.
713 Hydrological Processes 6(3): 279–298. http:///doi/abs/10.1002/hyp.3360060305
714 Chen J, ST-Denis B G, Brissette F P, Lucas-Picher P (2016) Using Natural Variability as a Baseline to Evaluate the
715 Performance of Bias Correction Methods in Hydrological Climate Change Impact Studies. American
716 Meteorological Society 17: 2155-2173. https://doi: 10.1175/JHM-D-15-0099.1
717 Chawla I, Mujumdar P P (2018) Partitioning uncertainty in streamflow projections under nonstationary model
718 conditions. Advances in Water Resources 112: 266-282. https://doi.org/10.1016/j.advwatres.2017.10.013
719 Chen S T, Yu P S, Tang Y H (2010) Statistical downscaling of daily precipitation using support vector machines
720 and multivariate analysis. Journal of Hydrology 385(1-4): 13-22. https: doi:10.1016/j. jhydrol.2010.01.021
721 Champagne O, Arain M A, Leduc M, Coulibaly P, McKenzie S (2020) Future shift in winter sreamflow modulated
722 by the internal variability of climate in southern Ontario. Hydrology and Earth System Sciences 24: 3077-3096.
723 Deser C, Phillips A, Bourdette V, Teng H M (2012) Uncertainty in climate change projections: the role of internal
724 variability, Climate Dynamic 38:527-546. http://doi 1007/s00382-010-0977-x
725 Deser C, Phillips A, Alexander M A, Smoliak B V (2014) Projecting north American climate over next 50 years:
726 uncertainty duo to internal variability. http://doi 10.1175/JCLI-D-13-00451.1
727 Doi Van, Kim M. J (2020) Projections on climate internal variability and climatological mean at fine scales over
728 South Korea. Stochastic Environmental Research and Risk Assessment 34(7): p. 1037-1058.
729 https://doi.org/10.1007/s00477-020-01807-y

730 Evin G, Hingra B, Blanche, J Eckert N, Morin, Verfaillie (2019) Partitioning Uncertainty Components of an
731 Incomplete Ensemble of Climate Projections Using Data Augmentation. Jounal of Climate 32:2423-2440.
732 https://doi. 10.1175/JCLI-D-18-0606.1
733 Ficklin D L, Letsinger S L, Stewart I T, Maurer E P (2016) Assessing differences in snowmelt-dependent
734 hydrologic projections using CMIP3 and CMIP5 climate forcing data for the western United States. Hydrology
735 Research 47: 483-500. https://doi: 10.2166/nh.2015.101.
736 Frankcombe L M, England M H (2015) Separating Internal Variability from the Externally Forced Climate
737 Response. Journal of Climate. 28: 8184-8202. https://doi: 10.1175/JCLI-D-15-0069.1
738 Gupta A, Govindaraju R S (2019) Propagation of structural uncertainty in watershed hydrologic models. Journal of
739 Hydrology 575: 66-81. https://doi.org/10.1016/j.jhydrol.2019.05.026
740 Galavi H, Mirzaei M (2020) Analyzing Uncertainty Drivers of Climate Change Impact Studies in Tropical and
741 Arid Climates. Water Resources Management 34: 2097-2109. https://doi.org/10.1007/s11269-020-02553-0
742 Hawkins E, Sutton R (2009) The potential to narrow uncertainty in regional climate predictions. American
743 Meteorological Society 90(8):1095-1108. https://doi.10.1175/2009bams2607.1
744 Hawkins E, Sutton R (2011) The potential to narrow uncertainty in projections of regional precipitation change.
745 Climate Dynamic 37: 407-418. http://doi 10.1007/s00382-010-0810-6
746 Hingray B, Blanchet J, Evin G, Vidal J P (2019) Uncertainty component estimates in transient climate projections:
747 Precision of estimators in a single time or time series approach. Climate Dynamic 4635-1.
748 https ://doi.org/10.1007/s0038 2-019-04635 -1
749 Kujawa H, Kalcic M, Martin J, Aloysius N, Apostel A, Kast J, Murumkar A, Evenson G, Becker R, Keller L,
750 Zischg A P, Mosimann M, Rössler O, Weingartner R, Martius O (2019) Large ensemble flood loss modelling and
751 uncertainty assessment for future climate conditions for a Swiss pre-alpine catchment. Science of The Total
752 Environment 693:133400. https://doi.org/10.1016/j.scitotenv.2019.07.206
753 Keller, L., Zischg, A. P., Mosimann, M., Rössler, O., Weingartner, R., & Martius, O. (2019). Large ensemble flood
754 loss modelling and uncertainty assessment for future climate conditions for a Swiss pre-alpine catchment. Science
755 of The Total Environment.693: 133400 https://doi:10.1016/j.scitotenv.2019.07.206.
756 Kim J, Tanveer M E, Bae D H (2018) Quantifying climate internal variability using an hourly ensemble generator
757 over South Korea. Stochastic Environmental Research and Risk Assessment 32:3037–3051.
758 https://doi.org/10.1007/s00477-018-1607-0
759 Li L, Diallo I, Xu C Y, Stordal F (2015) Hydrological projections under climate change in the near future
760 byRegCM4 in Southern Africa using a large-scale hydrological model. Journal of Hydrology 528:1-16.
761 http://dx.doi.org/10.1016/j.jhydrol.2015.05.028
762 Liu Y, Zhang J Y, Wang G Q, Liu J F, He R M, Wang H J, Liu C S, Jin J L (2012) Assessing the effect of climate
763 natural variability in water resources evaluation impacted by climate change. Hydrological Processes
764 27(7):1061-1071. https://doi: 10.1002/hyp.9251.
765 Lee M H, Bae D H (2016) Uncertainty Assessment of Climate Change Impacts on Hydrology: A Case Study for
766 the Central Highlands of Vietnam. Procedia Engineering 154: 617-623. https://doi: 10.1016/j.proeng.2016.07.560.
767 Lafaysse M, Hingray B, Mezghani A, Gailhard J, Terray L (2014) Internal variability and model uncertainty
768 components in future hydrometeorological projections: The Alpine Durance basin. Water Resources Research
769 50(4): p. 3317-3341. https:// doi:10.1002/ 2013WR014897
770 Maher N, Lehner F, Marotzke J (2020) Quantifying the role of internal variability in the temperature we expect to
771 observe in the coming decades. Environmental Research Letters 15:054014.
772 https://doi.org/10.1088/1748-9326/ab7d02
773 Nie W, Yuan Y P, Kepner W, Nash M S, Jackson M, Erickson C (2011) Assessing impacts of Land use and

774 Landcover changes on hydrology for the upper San Pedro watershed. Journal of Hydrology 407:105-114.
775 https://doi:10.1016/j.jhydrol.2011.07.012.
776 Nóbrega M T, Collischonn W, Tucci C E M, Paz A R (2011) Uncertainty in climate change impacts on water
777 resources in the Rio Grande Basin, Brazil. Hydrology and Earth System Sciences 15: 585-595.
778 https://doi:10.5194/hess-15-585-2011
779 Nerantzaki S D, Efstathiou D, Giannakis G V, Kritsotakis M, Grillakis M G, Koutroulis A G, Tsanis I K, Nikolaidis,
780 N P (2019) Climate change impact on the hydrological budget of a large Mediterranean island. Hydrological
781 Science Journal 6 :1190-1203. https://doi.org/10.1080/02626667.2019.1630741
782 Nerantzaki, S D, Hristopulos, D,T, Nikolaidis, N, P (2020) Estimation of the uncertainty of hydrologic predictions
783 in a karstic Mediterranean watershed. Science of the Total Environment 717:
784 137131 .https://doi.org/10.1016/j.scitotenv.2020.137131
785 Pesce M, Critto A, Torresan S, Giubilato E, Pizzol L, Marcomini A (2019) Assessing uncertainty of hydrological
786 and ecological parameters originating from the application of an ensemble of ten global-regional climate model
787 projections in a coastal ecosystem of the lagoon of Venice, Italy. Ecological Engineering 133:121-136.
788 https://doi.org/10.1016/j.ecoleng.2019.04.011
789 Qin X S, LU Y (2014) Study of climate change impact on flood frequencies_ A combined weather generator and
790 hydrological modeling approach. Journal of Hydrometeorology, 15(3):1205-12199.
791 https://10.1175/jhm-d-13-0126.1
792 Qi W, Zhang C, Fu G T, Zhou H C, Liu J G (2016) Quantifying Uncertainties in Extreme Flood Predictions
793 under Climate Change for a Medium-Sized Basin in Northeastern China. Journal of Hydrometeorology 17:
794 3099-3112. https://doi: 10.1175/JHM-D-15-0212.1.
795 Shi L, Feng P Y, Wan B, Liu D L, Cleverly J, Fang Q X, Yu Q (2020) Projecting potential evapotranspiration
796 change and quantifying its uncertainty under future climate scenarios: A case study in southeastern Australia.
797 Journal of Hydrology 584:124756. https://doi.org/10.1016/j.jhydrol.2020.124756.
798 Shen M, Chen J, Zhuan M J, Chen H, Xu C Y, Xiong L H (2018) Estimating uncertainty and its temporal variation
799 related to global climate models in quantifying climate change impacts on hydrology. Journal of Hydrology 556:
800 10-24. https://doi.org/10.1016/j.jhydrol.2017.11.004.
801 Schindler A, Toreti A, Zampieri M, Scoccimarro E, Gualdi S, Fukutome S F, Xoplaki E, Luterbacher J (2015) On
802 the Internal Variability of Simulated Daily Precipitation, Journal of Climate 28: 3624-3630.
803 http://dx.doi.org/10.1175/JCLI-D-14- 00745.s1.
804 Steinschneider, S, Wi S, Brown, C (2015) The integrated effects of climate and hydrologic uncertainty on future
805 flood risk assessments. Hydrological Processes, 29(12): 2823–2839. https://doi:10.1002/hyp.10409
806 Thompson W J D, Barnes, E A, Deser C, Foust W E, Phillips, A S (2015) Quantifying the Role of Internal Climate
807 Variability in Future Climate Trends.Journal of Climate, 28(16): 6443–6456. doi:10.1175/jcli-d-14-00830.1
808 Vaghef A S, Iravani M, Sauchyn D, Andreichuk Y, Goss G, Faramarzi M (2019) Regionalization and
809 parameterization of a hydrologic model significantly affect the cascade of uncertainty in climate-impact
810 projections. Climate Dynamics 53:2861-2886. https://doi.org/10.1007/s00382-019-04664-w.
811 Wang Q, XuY P, Xu Y, Wu L, Wang Y F, Han L F (2018) Spatial hydrological responses to land use and land
812 cover changes in atypical catchment of the Yangtze River Delta region. Catena 170:305-315.
813 https://doi.org/10.1016/j.catena.2018.06.022.
814 Wang Q, Xu Y P, Wang Y F, Zhang Y Q, Xiang J, Xu Y, Wang J (2020) Individual and combined impacts of future
815 land-use and climate conditions on extreme hydrological events in a representative basin of the Yangtze River
816 Delta, China. Atmospheric Research 23:104805. https://doi.org/10.1016/j.atmosres.2019.104805.
817 Wu H B, Chen (2015) Evaluating uncertainty estimates in distributed hydrological modeling for the Wenjing River

818 watershed in China by GLUE, SUFI-2, and ParaSol methods. Ecological Engineering 76:110-121
819 http://dx.doi.org/10.1016/j.ecoleng.2014.05.014.
820 Wang B, Liu D L, Waters C, Yu Q (2018) Quantifying sources of uncertainty in projected wheat yield changes
821 under climate change in eastern Australia. Climatic Change 151(2): 259273. https://doi.org/10.1007/s10584-018-
822 2306-z.
823 Wang F, Huang H G, Fan Y, Li Y P (2020) Robust Subsampling ANOVA Methods for Sensitivity Analysis of
824 Water Resource and Environmental Models. Water Resources Management 34: 3199-3217.
825 https://doi.org/10.1007/s11269-020-02608-2.
826 Xue C, Chen B, ASCE M, Wu H J (2014) Parameter Uncertainty Analysis of Surface Flow and Sediment Yield in
827 the Huolin Basin, China. American Society of Civil Engineers 19: 1224-1236. https://doi:
828 10.1061/(ASCE)HE.1943-5584 .0000909.
829 Yen H, Wang XY, Fontane D G, Harmel R D, Arabi M (2014) A framework for propagation of uncertainty
830 contributed by parameterization, input data, model structure, and calibration/validation data in watershed modeling.
831 Environmental Modelling & Software 54: 211-221. http://dx.doi.org/10.1016/j.envsoft.2014.01.004.
832 Yu B, Li G L, Chen, S F, Lin H (2020) The role of internal variability in climate change projections of North
833 American surface air temperature and temperature extremes in CanESM2 large ensemble simulations. Climate
834 Dynamics 55:869-885. https://doi.org/10.1007/s00382-020-05296-1
835 Yuan S S, Quiring S M, Kalcic M M, Apostel A M, Evenson G R, Kujawa H A (2020) Optimizing climate model
836 selection for hydrological modeling:A case study in the Maumee River basin using the SWAT. Journal of
837 Hydrology 588:125064. https://doi.org/10.1016/j.jhydrol.2020.125064
838 Zhang Y Q, You Q L, Chen C C, Ge J (2016) Impacts of climate change on streamflows under RCP scenarios: A
839 case study in Xin River Basin, China. Atmospheric Research 178-179:521-534.
840 http://dx.doi.org/10.1016/j.atmosres.2016.04.018.
841 Zhang R, Corte-Real J, Moreira M, Kilsby C, Birkinshaw S, Burton A, Fowler H J, Forsythe N, Nunes J P,
842 Sampaio, E, dos Santos F L, Mourato S (2019) Downscaling climate change of water availability, sediment yield
843 and extreme events_ application to a Mediterranean climate basin, International Journal of Climatology
844 39:2947-2963. https://doi: 10.1002/joc.5994.
845 Zhu X P, Zhang C, Qi W, Cai W J, Zhao X H, Wang X F (2018) Multiple Climate Change Scenarios and Runoff
846 Response in Biliu River. Water 10(2):690. https://doi:10.3390/w10060690.
847 Zhang L M, Yuan F, Wang B, Ren L L, Zhao C X, Shi J Y, Liu Y, Jianf S H, Yang X L, Chen T, Liu S Y(2021)
848 Quantifying uncertainty sources in extreme flow projections for three watersheds with different climate features in
849 China. Atmospheric Research 249:105331. https://doi.org/10.1016/j.atmosres
850
851
852
853
854